Enantiospecific Adsorption of Chiral Molecules on Chiral Gold Clusters

Xóchitl López-Lozano, Luis A. Pérez, and Ignacio L. Garzón

Instituto de Física, Universidad Nacional Autónoma de México, Apartado Postal 20-364, 01000 México D.F., México
(Received 29 April 2006; published 6 December 2006)

Enantioselectivity in gold clusters is investigated by studying the adsorption of a chiral amino acid (cysteine) on a chiral Au_{55} cluster using density functional calculations. The highest adsorption energies were found when the amino and thiolate functional groups of cysteine are bonded to the lowest coordinated edges of the chiral cluster. Enantiospecific adsorption is primarily obtained from the different bond location and strength, at the cluster edge, of the carboxyl groups forming the left- and right-handed enantiomers. These results provide theoretical support to convey enantioselectivity in asymmetric nano-catalysts using chiral gold clusters.

Chiral structures have been found as the lowest energy configurations of bare Au_{28} and Au_{55} and thiolate-passivated $Au_{28}(SCH_3)_{16}$ and $Au_{38}(SCH_{34})_{24}$ clusters from density functional theory (DFT) calculations [1–3]. These results provided theoretical support for the existence of chirality in metal clusters, suggested by the intense optical activity measured on size-separated glutathione-passivated gold clusters in the size range of 20–40 Au atoms [4] and, more recently, on penicillamine-passivated gold clusters with metal core mean diameters of 0.57, 1.18, and 1.75 nm [5]. On the other hand, photoelectron spectroscopy (PES) measurements of size-selected bare gold cluster anions indicated the formation of low-symmetry Au_{55}^- [6] and amorphouslike Au_{32}^- [7] isomers. Preliminary data from trapped ion electron diffraction (TIED) also show that only local order having fivefold symmetry exists in cationic and anionic Au_{55} and Au_{32} clusters [8], similar to the results observed in Ag_m^+ clusters [9]. The existence of disordered (low-symmetry) isomers in Au clusters in this size range had been theoretically predicted and interpreted as global or low-lying local minima of their potential energy surface [10,11]. A further structural analysis, using the Hausdorff chirality measure (HCM), as well as a semi-classical calculation of the circular dichroism spectrum, has shown that many of these disordered Au cluster isomers are chiral [1–3].

Enantioselectivity, i.e., the ability to distinguish between enantiomers in catalytic reaction processes, is a fundamental property of many organic and biological molecules. By an appropriate understanding and control of this property, important implications in molecular biology and in the pharmaceutical, food, and agricultural industries are expected [12]. The main objective is to find a chiral system that is able to separate from a racemic mixture of chiral molecules one specific enantiomer (with a single handedness *L* or *D*), which is the active molecule for the application of interest. Recent theoretical [13] and experimental [14] studies on intrinsic [15] and adsorbate driven [16] chiral metal surfaces have demonstrated the existence of enantioselective adsorption of chiral molecules when they are adsorbed on kink sites,

suggesting their use as heterogeneous asymmetric catalysts.

In this Letter, we study the capability of chiral Au clusters to induce enantioselective reactions with chiral molecules. Although several theoretical and experimental studies showed that supported and unsupported Au clusters are catalytically active for the oxidation of CO and other reactions [17], they have not yet been considered as enantioselective catalysts. In this work, we report the first theoretical study of the enantiospecific adsorption of a chiral amino acid (cysteine) on a chiral Au_{55} cluster using DFT, within the generalized gradient approximation (GGA). Our results show differences of ~ 100 meV in the adsorption energies of the right-handed enantiomer (*D*-cys) and the left-handed one (*L*-cys) when they adsorbed at the two lowest coordinated edges of this cluster, indicating that the chiral Au_{55} cluster leads to enantiospecific adsorption. This prediction suggests that chiral Au clusters might be used to design asymmetric nanocatalysts.

To investigate enantioselectivity in chiral gold clusters, we use the lowest energy isomer of Au_{55} obtained by combining a global optimization technique with a semi-empirical many body potential and a further local relaxation using DFT-GGA [1–3]. The index of chirality of this cluster, using HCM [1], was found to be HCM = 0.088. For comparison, the chiral fullerenes D_2-C_{76} and D_2-C_{84} have HCM = 0.109 and 0.102, respectively [1]. Two views of the geometry of this chiral cluster are shown in Figs. 1(a) and 1(b). The surface of this cluster is composed of several quasiplanar facets, most of them reminiscent of (111) planes. The largest facet has a 9-atom rhombic shape, as highlighted in Figs. 1(a) and 1(b) with a different color. Note the two lowest coordinated edges formed by three Au atoms with coordination numbers $N_c = 4$, 7, and 7. Figures 1(c) and 1(d) show the theoretical diffraction intensity of the cationic Au_{55}^+ cluster and the electronic density of states of the anionic Au_{55}^- one, respectively, obtained after relaxation using the structure of the neutral chiral Au_{55} cluster. Since the relaxed geometry of the charged Au_{55} clusters shows negligible variations with respect to the neutral cluster shown in Figs. 1(a) and
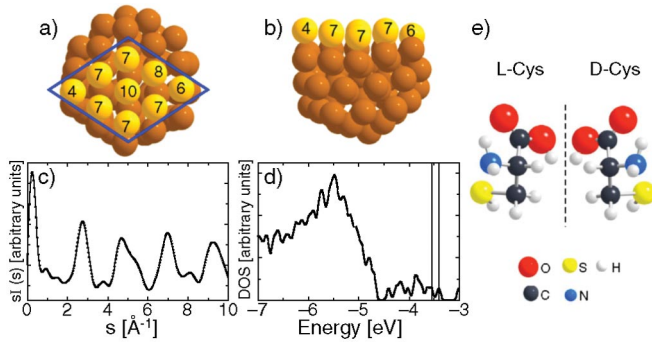
FIG. 1 (color). (a) Top and (b) side views of the most stable chiral Au_{55} cluster. Coordination numbers are displayed for the Au atoms forming the largest cluster facet with a rhombic shape. (c) Diffraction intensity of the chiral Au_{55}^{+} cluster. (d) Electronic DOS of the chiral Au_{55}^{-} cluster. (e) Geometric structure of *L*- and *D*-cysteine.

1(b), these results are useful for the experimental characterization of the chiral Au_{55} cluster using, for example, TIED [8,9] and PES [6]. Interestingly, there is experimental evidence on the existence of chiral gold clusters with around 55 atoms, as reported by Yao *et al.* [5].

Cysteine, one of the 20 amino acids building the most common proteins, is a chiral molecule with HCM = 0.191 in gas phase, and its two enantiomers are displayed in Fig. 1(e). Its three functional groups, thiol (SH), amino (NH$_2$), and carboxyl (COOH) can induce different adsorption modes with the chiral Au_{55} cluster. The adsorption modes of cysteine on the (111) surface of bulk gold have been studied [18], and its enantioselectivity upon adsorption on the chiral Au(17 11 9)^s surface has been demonstrated [15]. According to these studies, performed within DFT-GGA, the adsorption energies of cysteine on Au surfaces are of ~2 eV, whereas the adsorption energy difference between the *D*- and *L*-cys is of 140 meV [15].

The DFT-GGA calculations were done using the first-principles SIESTA code [19] with standard norm-conserving scalar-relativistic pseudopotentials [20], and the Perdew, Burke, and Ernzerhof exchange-correlation functional [21]. This methodology has been used by our group to predict the structural distortion of gold clusters upon thiol passivation [22]. By using another DFT approach, this prediction has been confirmed [23]. This agreement is a good indicator of the reliability of our calculations. Since the cysteine-Au_{55} cluster compound has a complex potential energy surface, the adsorption sites on which the amino acid adsorbs more strongly were obtained after an extensive search over more than 100 sites on all of the cluster facets. It is worth mentioning that the chiral Au_{55} cluster is slightly relaxed upon cysteine adsorption, increasing its HCM to values in the range of 0.091–0.101, depending on the location of the adsorption site.

The higher adsorption energies [24] were systematically obtained when the thiolate and amino groups of the cysteine were both adsorbed at the two lowest coordinated edges of the 9-atom rhombic facet of the chiral Au_{55} cluster. The most favorable site (that one for which the adsorption energy is the highest one) for the adsorption of *L*-cys was found at one of the lowest coordinated edges, formed by the three Au atoms labeled as Au(1), Au(2), and Au(3) (edge I), as shown in Figs. 2(a) and 2(c). *D*-cys also adsorbs strongly at edge I on the site depicted in Figs. 2(b) and 2(d). Likewise, the most favorable site for the adsorption of *D*-cys was found at the edge formed by the Au(1), Au(4), and Au(7) atoms (edge II), on the site displayed in Figs. 2(f) and 2(h). Figures 2(e) and 2(g) show the corresponding most stable configuration of *L*-cys when is adsorbed at edge II. The values of the calculated adsorption energies for *L*- and *D*-cys adsorbed at edges I and II are reported in Table I. They indicate that there exists enantiospecific binding when the cysteine adsorbs at the edges of the chiral Au_{55} cluster: at edge I in favor of *L*-cys by 102 meV and at edge II in favor of *D*-cys by 129 meV. It is remarkable that these differences in adsorption energies are comparable to that obtained when this amino acid is adsorbed on a chiral Au surface (140 meV) [15]. On the other hand, if enantioselectivity is related to the difference in adsorption energies between the most favorable adsorption sites of *L*-cys and *D*-cys, wherever they are located on the cluster surface, our results show that *D*-cys adsorbs more strongly at edge II than *L*-cys at edge I by 58 meV. Again, this result is comparable to that obtained using the lowest energy configurations of the APPT chiral molecule adsorbed on the chiral Au(17 11 9)^s surface (91 meV) [13].

The adsorption modes of both enantiomers in the most favorable configurations are characterized by the binding of the amino group to the lowest coordinated vertex Au(1) atom on a top site. This amino-gold interaction does not require dehydrogenation but is caused by the electronic
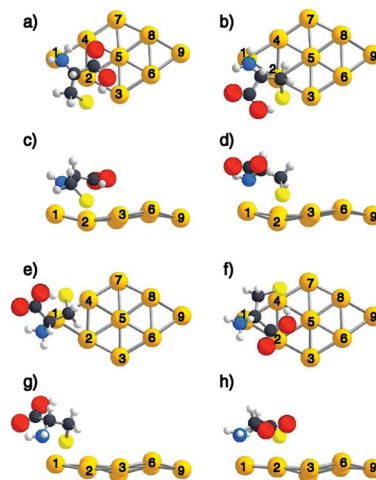

FIG. 2 (color). Top and side views of the lowest energy structures of cysteine adsorbed on the chiral Au_{55} cluster (only the 9 Au atoms forming the cluster rhombic facet are displayed and labeled 1–9). (a),(c) *L*-cys at edge I. (b),(d) *D*-cys at edge I. (e),(g) *L*-cys at edge II. (f),(h) *D*-cys at edge II.

TABLE I. Adsorption energies (eV) and bond distances (Å) of L- and D-cys adsorbed at edges I (Au1-Au2-Au3) and II (Au1-Au4-Au7) of the chiral Au_{55} cluster. ΔE_{ads} (eV) is the difference in the adsorption energies between L- and D-cys.

	L-cys	D-cys			ΔE_{ads}
$E_{ads}^{edge\ I}$	−1.581		−1.479		−0.102
$E_{ads}^{edge\ II}$	−1.510		−1.639		0.129
Edge I	L-cys	D-cys	Edge II	L-cys	D-cys
d_{Au1-N}	2.408	2.388	d_{Au1-N}	2.484	2.351
d_{Au2-S}	2.470	2.497	$d_{Au1/4-S}$	2.568	2.440
d_{Au3-S}	2.844	2.550	$d_{Au4/7-S}$	2.506	3.645
d_{N-S}	3.911	3.725	d_{N-S}	3.245	3.925
$d_{Au4/1-O}$	3.128	4.326			
$d_{Au5/2-O}$	3.280	5.390			
$d_{Au3/2-O_H}$	3.239	5.038			
$d_{Au5/3-O_H}$	3.382	5.427			
$d_{Au2/1-C}$	3.366	4.197			
$d_{Au5/2-C}$	3.487	4.692			

hybridization of the N and Au orbitals, as was discussed in Ref. [18]. In the binding of the thiolate group, two different nearly top sites are involved. For L-cys, the sulfur atom is closer to the Au(2) atom at edge I [see Figs. 2(a) and 2(c)], whereas for D-cys, the S atom is on top of the Au(4) atom at edge II [see Figs. 2(f) and 2(h)]. Figures 2(b) and 2(d) display the D-cys when it is adsorbed at edge I. In this case, the adsorption mode is similar to the one discussed above for L-cys, although the thiolate group of D-cys is now closer to a bridge site at edge I, involving the Au(2) and Au(3) atoms. In the same way, L-cys preferentially adsorbs at edge II by the binding of the amino group on the top site, involving the Au(1) vertex atom, and through the thiolate group interacting mostly with the Au(4) atom, as is depicted in Figs. 2(e) and 2(g).

To understand the origin of enantiospecific adsorption of cysteine on the chiral Au_{55} cluster, it is useful to focus on the results of the adsorption of L- and D-cys at edge I. Although both enantiomers are adsorbed through the thiolate and amino groups in a similar configuration (Table I shows nearly equal bond distances for the gold-sulfur and gold-nitrogen atoms), the position and orientation of the carboxyl group relative to the 9-atom rhombic facet of the chiral cluster are definitively different. Table I shows that the bond distances between the carboxyl group atoms and the nearest Au atoms are much larger for D-cys than for L-cys. Figures 2(a)–2(d) also show that, for L-cys adsorbed at edge I, the carboxyl group is oriented inward and almost parallel to the cluster rhombic facet, whereas D-cys is oriented outward from the cluster rhombic facet. From these geometric arguments is evident that the position and orientation of the carboxyl group relative to the cluster edge is the key factor to explain the enantioselectivity. In fact, it was found that the adsorption energy of the D-cys does not increase if it is displaced inward, in such a way that the carboxyl group approaches the cluster surface. Although in this case the carboxyl-gold interaction could

gain some energy, it is not enough to compensate the loss due to breaking the bonds of the thiolate and amino groups at edge I. These calculations show that it is energetically more favorable to keep the bonding of the amino group close to the lowest coordinated vertex gold atom Au(1) and the thiolate one bonded to the remaining lowest coordinated Au atoms forming edge I. A trend emerging from these results indicates that, if both cysteine enantiomers maximize their adsorption energy through the bonding of the amino and thiolate groups at edge I, their intrinsic mirror symmetry necessarily place their carboxyl groups in inward (L-cys) and outward (D-cys) positions with respect to the cluster edge, leading to enantiospecific adsorption.

To estimate the energetic effect of the carboxyl group, the adsorption energies of the S, NH_2, and COOH groups alone were calculated from separate DFT-GGA calculations, as was proposed in Ref. [13]. These calculations show that, for the thiolate and amino groups alone, the difference in adsorption energy between the left- and right-handed enantiomeric groups is negligible, whereas the difference in the adsorption energies of the carboxyl groups is much larger. In the latter case, this larger difference occurs because the carboxyl group of D-cys has a weak repulsive interaction with the cluster surface, whereas for L-cys there exists an attractive bonding.

The contribution of the carboxyl group to enantioselectivity is also evident from the analysis of its density of states (DOS) and charge density distribution. Figures 3(a)– 3(d) show the DOS of the carboxyl group and the three Au atoms that are closer to this functional group: Au(3), Au(4), and Au(5) for L-cys and Au(1), Au(2), and Au(3) for D-cys. Figures 3(a) and 3(b) show that the number of electronic states coming from the carboxyl of L-cys is higher than in the case of D-cys, in the energy range where the s and d valence states of the gold atoms are present. This distinct electronic behavior induces a larger hybridization between the carboxyl orbitals of L-cys and the Au atoms. Such behavior is also evident in the energy range of the highest occupied molecular orbital–lowest unoccupied molecular orbital (HOMO-LUMO) gap, as shown in Figs. 3(c) and 3(d). Then the higher adsorption energy of L-cys at edge I can be associated to the larger orbital hybridization existing in this system. Moreover, Figs. 3(e) and 3(f) show different profiles in the charge density of the carboxyl group adsorbed at edge I, providing additional evidence of the distinct bond formation between each enantiomer and the chiral cluster. Although the previous discussion has been restricted to analyze how the different geometric, energetic, and electronic effects associated to the bonding of the carboxyl group explain the enantiospecific adsorption of cysteine at edge I, similar physical arguments can explain the adsorption modes leading to enantioselectivity at edge II.

The above results show that the physical origin of the enantiospecific adsorption in chiral clusters is qualitatively different from that obtained in extended chiral surfaces,
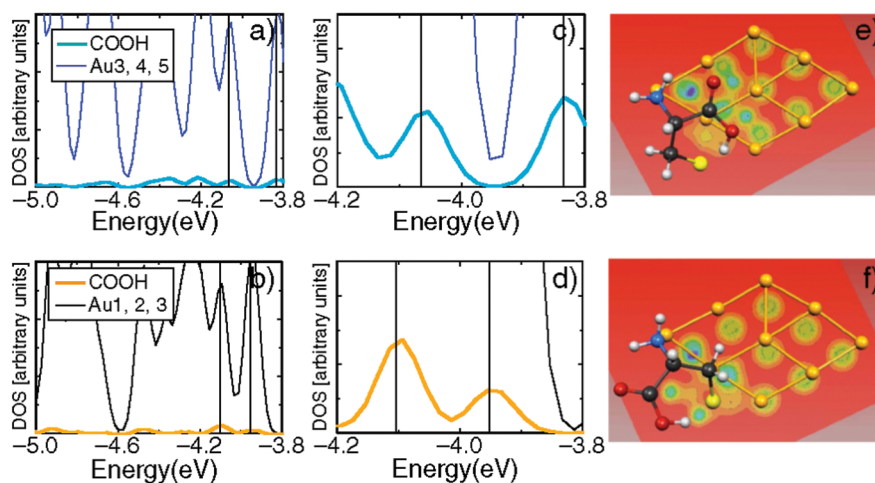
FIG. 3 (color). Projected DOS of the carboxyl group and their nearest Au atoms on the adsorption sites at edge I: (a),(c) for *L*-cys and (b),(d) for *D*-cys. (c) and (d) are a magnification in the region of the HOMO-LUMO gap. Contour charge density maps of the carboxyl group adsorbed on the cluster surface: (e) for *L*-cys and (f) for *D*-cys.

where the carboxyl group effect was found to be negligible [15]. It is encouraging that, recently, the importance of the carboxyl group interaction with a chiral gold cluster has been experimentally demonstrated [25], providing strong support for our predictions. In this way, the adsorption modes of *L*- and *D*-cys on the chiral Au$_{55}$ cluster could be helpful to design enantioselective chemical reactions involving the "hanging" carboxyl group that would be able to interact with other functional groups or molecules. Formation of peptide bonds [26] and asymmetric hydrogenation [27] are some examples of enantioselective reactions. In order to explore possible catalytic scenarios, chiral metal clusters covered with chiral molecules could be confined in ion traps and characterized by mass spectrometry [28] or prepared in solution, where chiroptical techniques such as circular dichroism and vibrational circular dichroism can be used [25].

In summary, the enantiospecific adsorption of cysteine on the chiral Au$_{55}$ cluster has been demonstrated from DFT-GGA calculations. Its physical origin is attributed to the different location and strength of the interaction of the cysteine functional groups, caused by the mirror symmetry existing between the left- and right-handed enantiomers, when they are adsorbed at the lowest coordinated edges of the chiral cluster. Then the driving force for enantioselectivity is related to the finite size of the adsorption "substrate," which in this case corresponds to the cluster facet, and to the different energetic contributions of the carboxyl group forming the *L*- and *D*-cys enantiomers. This behavior is expected to remain for supported clusters, since there is theoretical evidence indicating that the structural and electronic properties of gold clusters do not significantly change when they are deposited on a substrate [29]. Finally, it is worth mentioning that the synthesis and characterization of chiral gold clusters of different sizes [25,30] as well as chiral silver nanoparticles [31] has been reported, opening the possibility to perform enantiospecific adsorption studies on a wider class of chiral nanostructures.

[1] I. L. Garzón *et al.*, Phys. Rev. B **66**, 073403 (2002).
[2] I. L. Garzón *et al.*, Eur. Phys. J. D **24**, 105 (2003).
[3] C. E. Román-Velázquez, C. Noguez, and I. L. Garzón, J. Phys. Chem. B **107**, 12 035 (2003).
[4] G. T. Schaaff and R. L. Whetten, J. Phys. Chem. B **104**, 2630 (2000).
[5] H. Yao *et al.*, J. Am. Chem. Soc. **127**, 15 536 (2005).
[6] H. Häkkinen *et al.*, Phys. Rev. Lett. **93**, 093401 (2004).
[7] M. Ji *et al.*, Angew. Chem., Int. Ed. **44**, 7119 (2005).
[8] J. H. Parks *et al.* (to be published).
[9] X. Xing *et al.*, Phys. Rev. B **72**, 081405(R) (2005).
[10] I. L. Garzón and A. Posada-Amarillas, Phys. Rev. B **54**, 11 796 (1996).
[11] I. L. Garzón *et al.*, Phys. Rev. Lett. **81**, 1600 (1998).
[12] R. Raval, Nature (London) **425**, 463 (2003).
[13] Ž. Šljivančanin *et al.*, J. Am. Chem. Soc. **124**, 14 789 (2002).
[14] A. Kühnle *et al.*, J. Am. Chem. Soc. **128**, 1076 (2006).
[15] T. Greber *et al.*, Phys. Rev. Lett. **96**, 056103 (2006).
[16] J. I. Pascual *et al.*, J. Chem. Phys. **120**, 11 367 (2004).
[17] R. Meyer *et al.*, Gold Bulletin (London) **37**, 72 (2004).
[18] R. Di Felice and A. Selloni, J. Chem. Phys. **120**, 4906 (2004).
[19] J. M. Soler *et al.*, J. Phys. Condens. Matter **14**, 2745 (2002).
[20] N. Troullier and J. L. Martins, Phys. Rev. B **43**, 1993 (1991).
[21] J. P. Perdew *et al.*, Phys. Rev. Lett. **77**, 3865 (1996).
[22] I. L. Garzón *et al.*, Phys. Rev. Lett. **85**, 5250 (2000).
[23] H. Häkkinen *et al.*, J. Phys. Chem. B **110**, 9927 (2006).
[24] The adsorption energies were obtained from: $E_{ads} = E_{tot}(Au_{55} + Cys) - E_{tot}(Au_{55}) - \{E_{tot}(Cyc) - \frac{1}{2}E_{tot}(H_2)\}$.
[25] C. Gautier and T. Bürgi, J. Am. Chem. Soc. **128**, 11 079 (2006).
[26] E. R. Jarvo and S. J. Miller, Tetrahedron **58**, 2481 (2002).
[27] R. Noyori *et al.*, Proc. Natl. Acad. Sci. U.S.A. **101**, 5356 (2004).
[28] A. T. Iavarone *et al.*, Int. J. Mass Spectrom. **253**, 172 (2006).
[29] L. M. Molina and B. Hammer, J. Catal. **233**, 399 (2005).
[30] Y. Yanagimoto *et al.*, J. Phys. Chem. B **110**, 11 611 (2006).
[31] G. Shemer *et al.*, J. Am. Chem. Soc. **128**, 11 006 (2006).